The Elura Compendium

D. W. Emerson

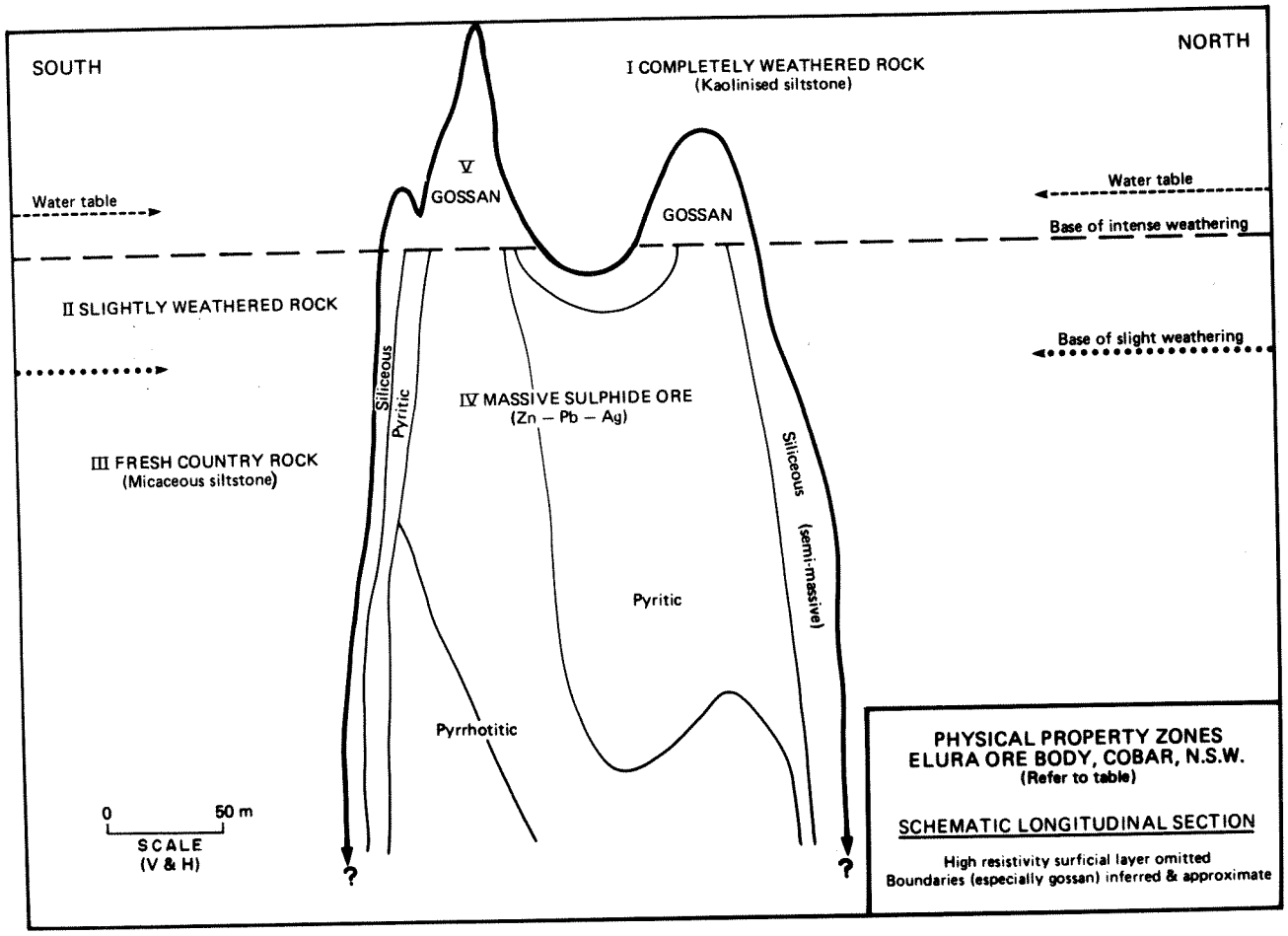

Estimated Average Bulk Physical Properties — Elura Orebody Zones	I Completely Weathered Country Rock	II Slightly Weathered Country Rock	III Fresh Country Rock	IV Sulphide Ore Si	IV Sulphide Ore Py	IV Sulphide Ore Po	V Gossan
Lithology	quartz kaolin sericite rock	quartz muscovite siltstone		semi massive to dissem siliceous	massive pyritic	massive pyrrhotitic	limonite
Weathering	intense	very slight	none	none	none	none	intense
Porosity, %, Total (Effective)	12 (7)	2 (0.3)	< 1		≪ 1		20 (11)
Permeability. cm/sec.	10^{-3} to 10^{-4} (fair to poor)	10^{-3} to 10^{-5} within 80 m of ore (∵ jointing), 10^{-7}			10^{-7} (impermeable)		10^{-1} to 10^{-2} (good)
Dry Bulk Density gm/cc.	2.3	2.7	2.75	3.7	4.5	4.4	3.0
Water Saturation, S_W%	50+(?)	100	100	0	0	0	≪50 (?)
Resistivity ohm m	10-20	500±	1500±	35	0.3	0.1	300±
Percent Frequency Effect (IP)	very small	minor	minor	220	25	15	small (?) at depth
Magnetic Susceptibility, cgs x 10^6	20	30	30	10	70	3000±	50
Koenigsberger Ratio, Q_n	0.1	0.1	0.1	0.1	0.1	5±	3
Velocity, V_p, m/sec	1200 – 4000	5000	5500		5600		4000 surface, 4300 @ depth

Continued

Geology of the Elura Zn-Pb-Ag Deposit

R.L. Adams & B.L. Schmidt

Electrolytic Zinc Co. of Australasia Ltd.,
P.O. Box 433, Cobar, N.S.W. 2835

Introduction

The Elura Zn-Pb-Ag deposit is situated 43km NNW of Cobar; the location and geology are shown in Figures 1 & 2.

The initial drill intersection at Elura was achieved in February 1974 following a phased programme of airborne and ground magnetics, bedrock geochemistry and I.P. surveys (refer Davis, 1980, for a more detailed history).

Elura is the northernmost known deposit in the Cobar mineral field, which has, since 1870, been an important gold and base metal producer. All the significant mineral deposits occur in the Cobar Super-Group, and general reference to the stratigraphy and mineralogy can be found in Andrews (1911), Rayner (1969), Robertson (1974) and Baker (1978).

Annual rainfall of approximately 300mm, supports ephemeral grasses and medium density scrub, below a sparse canopy dominated by acacia and eucalypts. The Elura deposit is situated in a gently undulating area of low relief. Surface drainage is by sheet flooding in broad drainage channels. Vehicle access to most of the area is good.

Reserves

Drilling has delineated a geological reserve of 27 million tonnes of Zn-Pb-Ag mineralisation from the base of oxidation at 100m to 510m below surface, with an average grade of 8.3% Zn, 5.6% Pb, 140gm/tonne Ag and less than 0.2% Cu. The average specific gravity of the deposit is 4.2 and of the host rock 2.65.

Geology

Mineralisation is hosted by a folded monotonous sequence of graded siltstones and shales belonging to the lower Devonian C.S.A. Siltstone unit of the Cobar Super-Group (Fig:2). There is almost no outcrop in the vicinity of Elura, the geology is known only from drill-hole data and shallow back-hoe pits. Bedrock is mantled by a thin (0.3-2m) regolith with up to 10m of unconsolidated alluvium present in drainage depressions. The top 0.5m of bedrock is normally iron-stained or ferruginised, with some local development of calcrete. Maghemite bearing gravels occur as older residual deposits on elevated areas or reworked into modern drainage features. The magnetic response of these gravels is observable on the aeromagnetic data. The C.S.A. Siltstone consists principally of quartz and muscovite with chlorite, albite, carbonate and accessory pyrite (normally 0.25-0.7%), rutile and approximately 0.1% kerogen-graphite. Weathering has produced a porous quartz-muscovite rock which is completely oxidised to a depth of between 75-105m. The weathered-fresh rock interface is gradational both macroscopically and microscopically over an interval of 12-36m.

The water table is horizontal and stands as a perched layer above the generally impermeable fresh siltstone 80-115m below surface, as shown on Figure 3. The water is highly saline, being essentially a Na-Cl brine with up to 1.9% total dissolved salts (Table 1). Cavities within the gossan and the sulphide mineralisation, below the water table depth of 80m, are not filled with water. Apparently, more intense fracturing and jointing in the vicinity of the contact be-

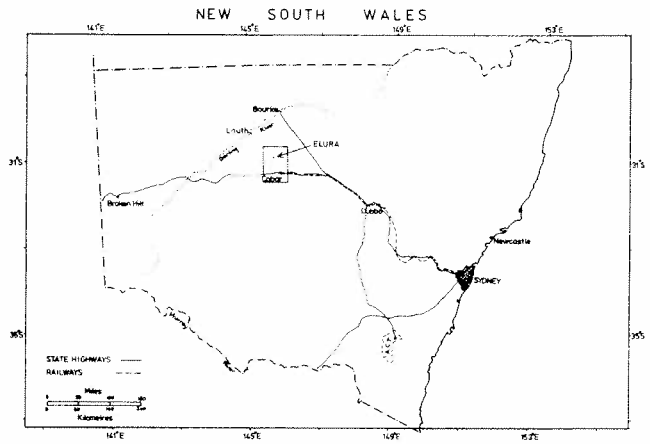

FIGURE 1
Locality plan Elura Deposit

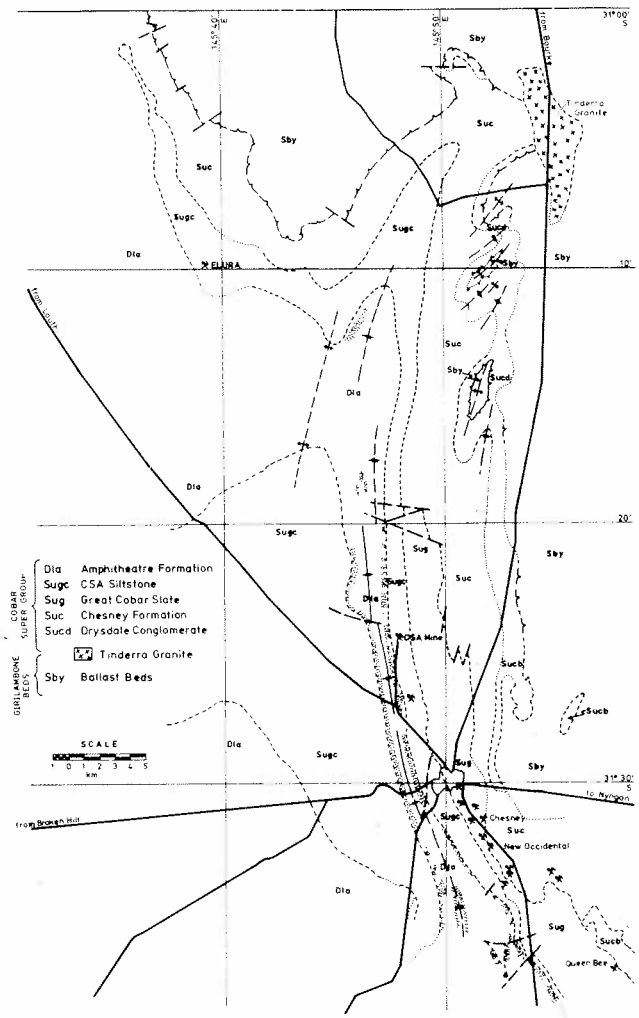

FIGURE 2
Regional geology Cobar area

tween host rock and mineralisation has allowed the ground water in the immediate vicinity of the deposit to percolate down to an unidentified lower aquifer. The gossan and host rock above the water table are not desiccated and contain sufficient moisture to ensure electrolytic conduction.

The contact between the mineralisation and the host C.S.A. Siltstones is generally abrupt. However, in some areas a gradational contact exists over 0.3-12m. A megascopic alteration halo comprised of minor sulphide and siderite porphyroblasts with local chloritisation occurs in a zone 5-70m wide around the mineralisation. The sulphide content of this halo rarely exceeds 3.0% by volume.

Ion		ppm
Bicarbonate	(HCO_3^-)	228
Sulphate	($SO_4^=$)	1083
Nitrate + Nitrite	(NO_X^-)	0.7
Calcium	(Ca^{++})	678
Magnesium	(Mg^{++})	950
Sodium	(Na^+)	5775
Potassium	(K^+)	65
Chloride	(Cl^-)	10,300
T.D.S.		19079.7 (1.91%)
Electrical Conductivity:		31 800 μ Siemens/cm 25°C i.e. 3.18 Siemens/m (3.18 mhos/m) (0.32 ohm m water resistivity)
pH		7.7

TABLE 1
Analysis of groundwater from Elura exploration shaft

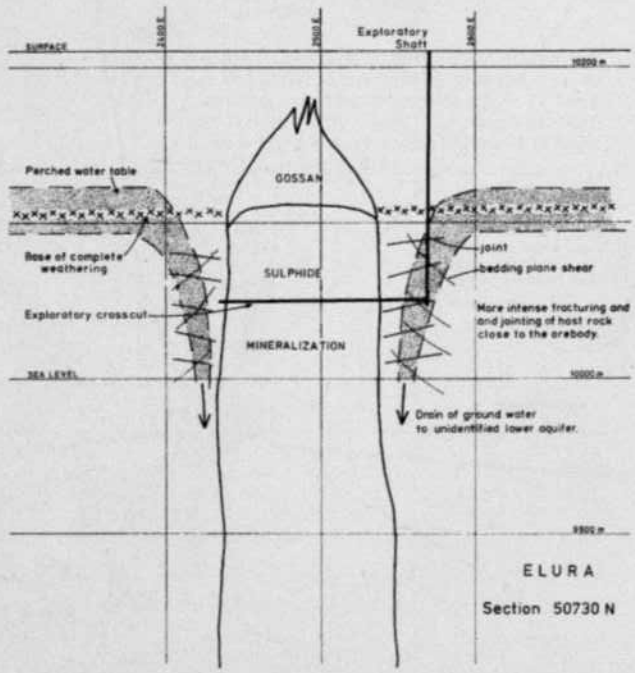

FIGURE 3
Section illustrating weathering and ground water distribution

Mineralisation

The orebody occurs as a discrete vertical pipe-like body in the core of an anticlinal or domal structure. The orebody is elongated north-south with maximum dimensions 200m x 120m. Drilling to date has delineated mineralisation to a depth of 500m (Fig: 4-8). Towards the top, the mineralisation divides into two apophyses which have been completely oxidised above 98m depth producing mature porous gossans containing numerous cavities, particularly near the base of the gossan. The southern gossan is the product of weathering of massive pyrrhotitic and pyritic mineralisation, while the northern gossan was originally composed of brecciated semi-massive siliceous mineralisation. The southern apophysis reaches the surface as a small area of gossan float. The gossan consists of goethite and haematite with mimetite, beudantite, coronadite and several minor minerals. A thin (2-4m thick) layer of Pb-Cu enriched supergene mineralisation has formed below the larger southern gossan peak.

The deposit can be subdivided into three major mineralisation types on the basis of mineralogy and specific gravity. Contacts between mineralisation types are generally distinct.

Siliceous Ore: This is semi-massive to disseminated mineralisation with a siliceous matrix. It contains from 20% to 50% by volume silica in various forms associated with pyrite, Fe-poor sphalerite, galena, minor arsenopyrite, chalcopyrite, tetrahedrite and siderite. Siliceous mineralisation is highly variable and includes brecciated laminated cherty,

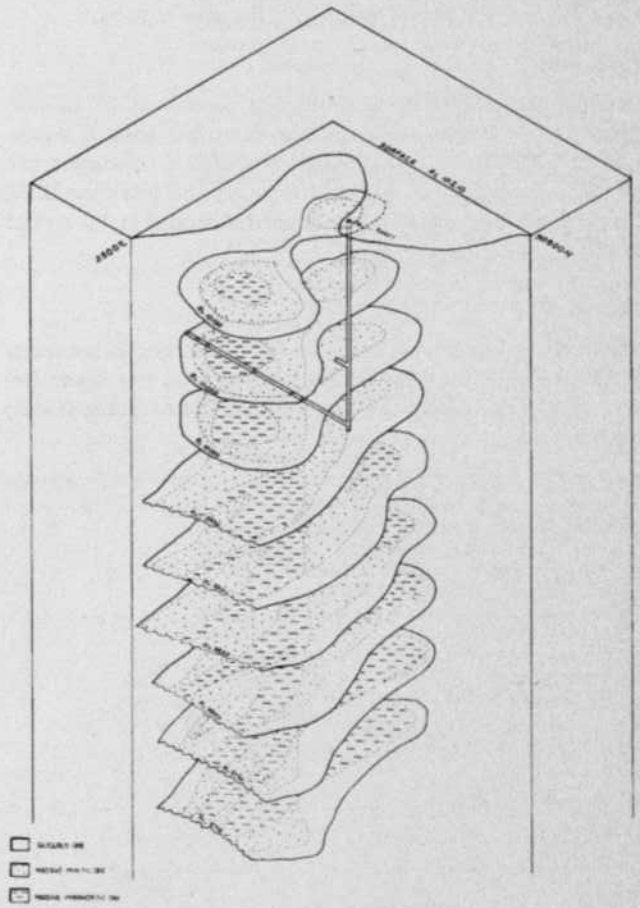

FIGURE 4
Isometric diagram of Elura ore body

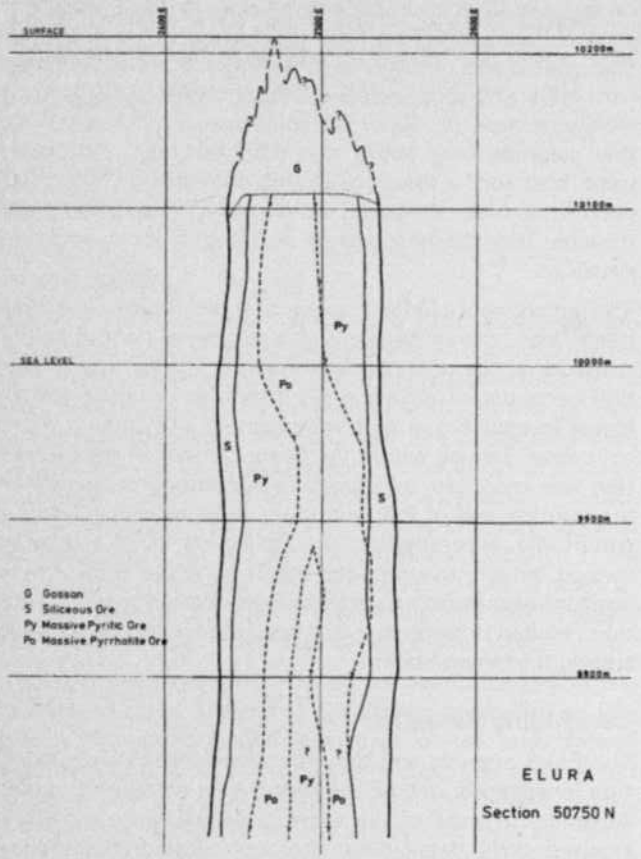

FIGURE 5
Cross section 50750 N. of the Elura ore body

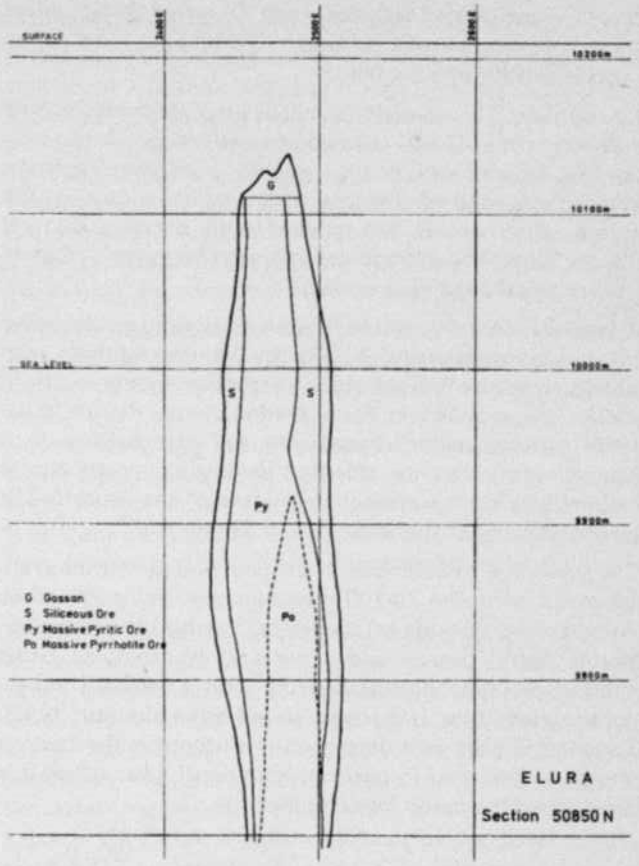

FIGURE 7
Cross section 50850 N. of the Elura ore body

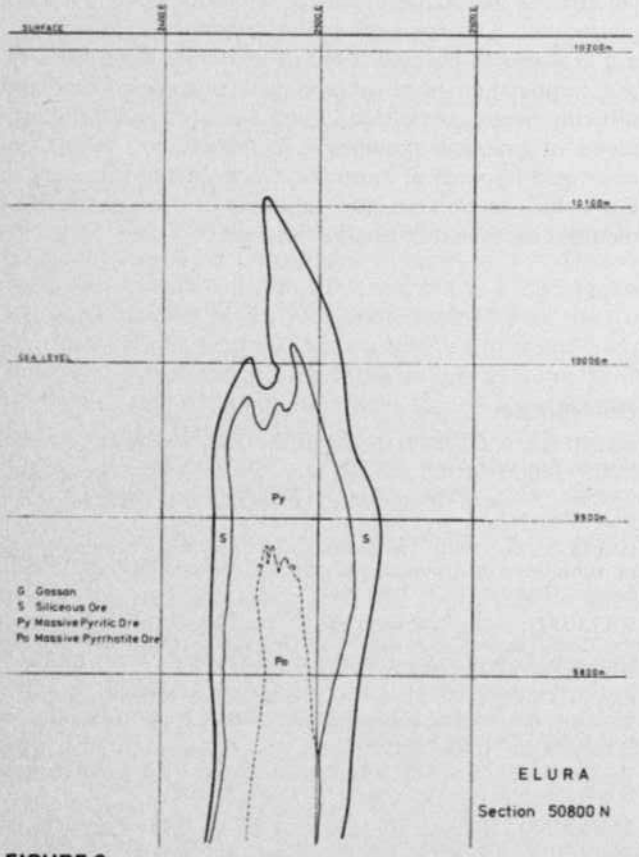

FIGURE 6
Cross section 50800 N. of the Elura ore body

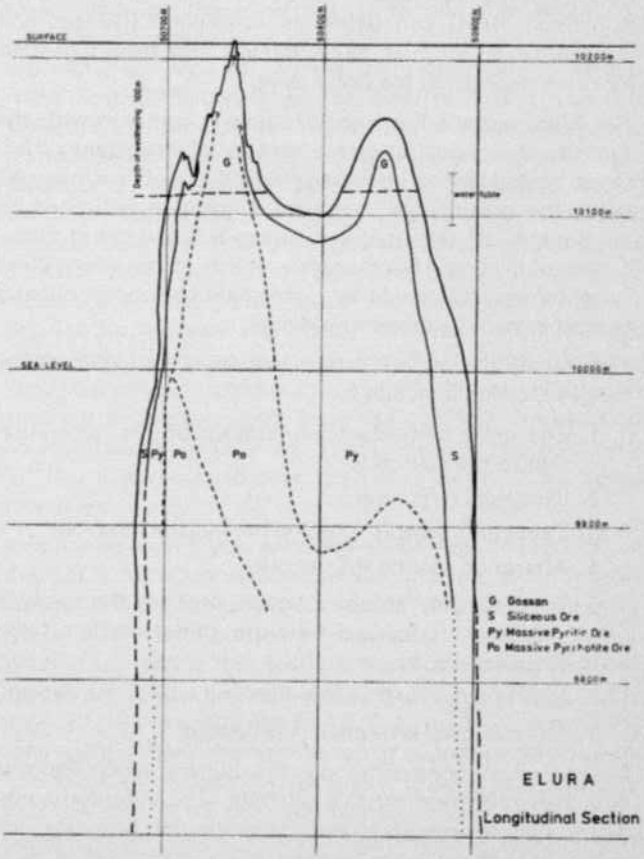

FIGURE 8
Longitudinal section Elura ore body

Gravity and Magnetic Surveys — Elura Orebody

G. Blackburn

Geology Department, University of Tasmania,
G.P.O. Box 252C,
Hobart, Tasmania 7001

Gravity and magnetic investigations prior to the discovery of the Elura field, at Cobar, Australia in 1974 indicated an anomalous body 250 m in length, 120 m in maximum width and a depth to the top of 90 m. The body dips 80° W and assuming a density contrast of 1600 kg/m^3 between mineral and host rock, the body would have a mass of 34.4 million tonnes. The interpretation presented compares well with the post drilling model.

Introduction

The gravity and magnetic surveys discussed in this paper were presented in the author's B.Sc. Honours thesis in 1974 and were completed prior to the drilling of the first discovery hole at the Elura prospect. While I.P., and resistivity techniques were also used, no discussion is presented in light of the more comprehensive surveys carried out by later workers. Electromagnetic measurements are briefly discussed. A full discussion of the integrated approach is contained in a further paper (Blackburn, 1980). *All discussions and results are those presented in 1974.*

Aeromagnetic Interpretation

Previous aeromagnetic surveys (e.g. Thomson, 1953 and Richardson & Keating, 1947) have produced very small (up to 40 nanoTesla [nT]) anomalies over the Cobar ore bodies.

During May, 1972, a low level (90 m) reconnaissance aeromagnetic survey was flown for the Electrolytic Zinc Company of A'asia Ltd. over their Cobar license. Results were accurate to 1 nT. Of fifteen selected anomalies only one, the Elura prospect was substantiated by later ground reconnaissance magnetics. The other anomalies were due to either a maghemite source on the ground surface or to stratigraphic layers.

The Elura anomaly occurs as a small 55 nT anomaly (Figure 1) on only one aeromagnetic profile. A regional gradient of 45 nT/1000 m has been removed to yield the anomalous field.

As only one magnetic profile intersects this anomaly the body is assumed to be equidimensional and considering the shape of other Cobar orebodies, curve fitting of a spherical body based on the assumption that the magnetic body is polarised by the earth's induction has been calculated.

Curve fitting (Figure 2) yields a depth of 250 m to the centre of the sphere below the ground surface. The radius of the sphere can also be determined providing the susceptibility of the material is known. It is assumed that the body is of similar composition to the nearby Cobar orebodies. Richardson & Keating (*op.cit.*) suggested an intensity of magnetisation for the New Cobar anomaly as 14 x 10^{-4} c.g.s. units. This value would yield a radius for the spherical source of 118 m — a value that is well in keeping with the known size of orebodies in the area.

Gravity Survey Techniques and Constraints

The use of gravity surveys for assessing metallic mineral deposits is well known. Their effectiveness is limited by the fact that gravity anomalies produced by large economic orebodies are small and thus easily masked by the effects of topographic irregularities, moderate variations in the thickness and composition of the overburden and regional anomaly trends due to relatively deep-seated masses.

Yungul (1956) illustrates the small magnitude of gravity anomalies obtained even on compact spherical ore masses (Figure 3). It is therefore imperative that the overall survey accuracy be maintained to an extremely high precision.

From December, 1973, until March, 1974, 374 stations were occupied with a Worden gravity meter. Readings were

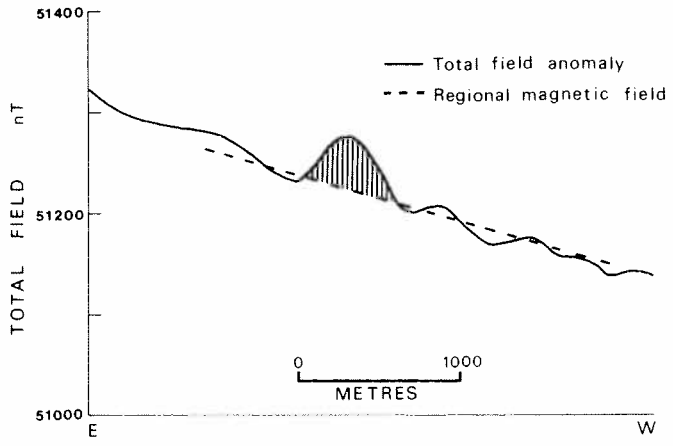

FIGURE 1

Total intensity air magnetic profile over the Elura prospect

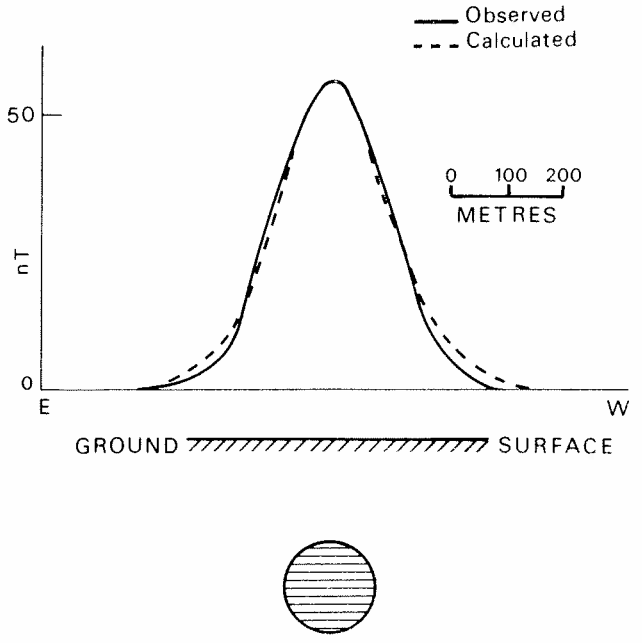

FIGURE 2

Comparison of theoretical and observed total field magnetic anomalies for a spherical source

recorded at 25 m intervals on a rectangular grid. Traverses on drift controlled loops normally consisted of 11 stations and loops were closed within an hour. The drift of the meter averaged 0.5 μG/hour.

The gravity network consists of a primary network of 57 tie stations which, when adjusted, are considered to be fixed when adjusting secondary networks. The adjustment of the network was computed using a least squares technique following Green (1961) who reduced the problem of calculating the above adjustments to one of solving "N" equations in "N" unknowns. The precision of the gravity data is half the r.m.s. misclosure or 0.4 μG.

The elevations of all stations were surveyed using a theodolite and adjusted by the least squares network technique used for the gravity data. After network adjustment, errors in elevations are equivalent to 0.2 μG.

Density variations below the earth's surface are a primary factor in the consideration of the magnitude and type of anomaly which might be caused by a geological structure and which might be detected by a gravity survey. The results of density determinations from freshwater saturated drill core samples are presented in Table 1.

TABLE 1

Saturated Rock Densities at Elura

Rock Type	Number of Samples	Density Range kg/m^3	Average kg/m^3
Host Rock			
– weathered	8	2190 – 2580	2430
– fresh	15	2650 – 2840	2760
Gossan	3	3340 – 3670	3480
Mineralised Zone	14	2870 – 4960	4210

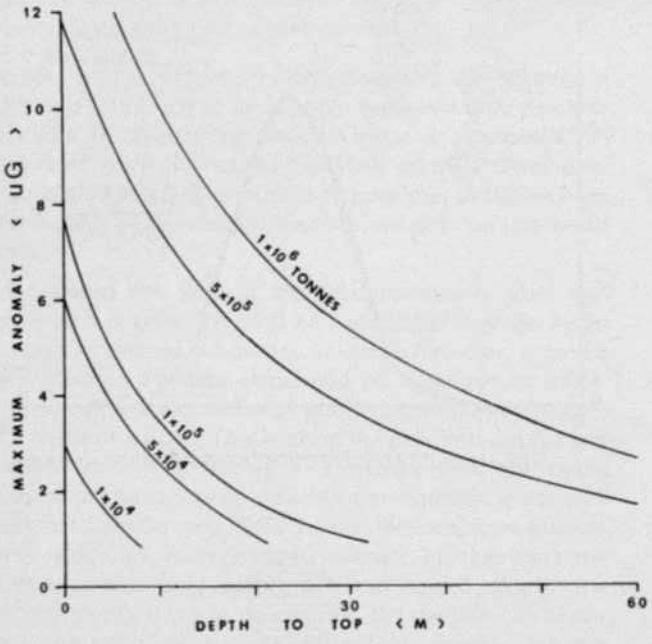

FIGURE 3

Maximum gravity anomaly due to spherical masses at different depths (after Yungal, 1956)

In the reduction of gravity data it is imperative that the density of the material between the geoid and the plane of observation be known.

Two mutually perpendicular Schlumberger electrical soundings were conducted at either end of the survey area (Figure 4) in order to elucidate the geophysical environment and depth of oxidation at the Elura prospect.

The similarity in form and level of the mutually perpendicular soundings (Figure 4) indicates relatively homogeneous conditions over the depth sounded. The Schlumberger data were interpreted using the method developed by Mooney et al. (1966) for resistivity computation over horizontally layered earth models. Interpretation reveals a conducting oxidised layer (6-13 ohm m) to a depth varying from 67 to 93 m overlying a resistive basement. A shallow, more resistive (40-60 ohm m) layer up to 3 m thick occurs near the surface.

Knowledge of the depths of weathering and the densities of weathered and fresh host rock suggested a Bouguer density of 2600 kg/m. No terrain corrections were applied since such corrections are much less than the errors due to topography and drift. The r.m.s. accuracy of the observations was 0.4 μG. The Bouguer anomaly is illustrated in Figure 5.

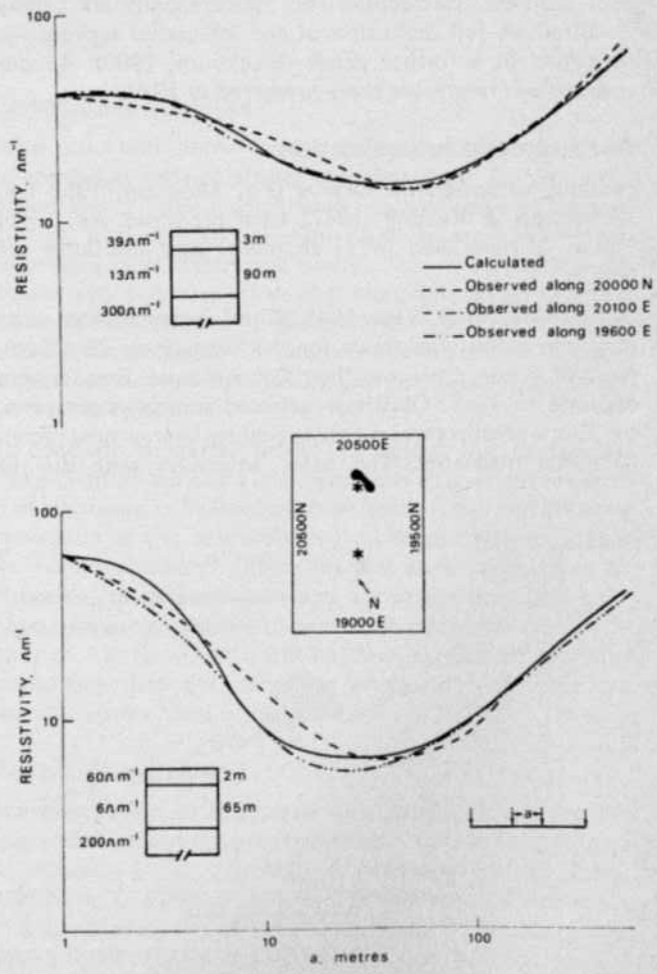

FIGURE 4

Comparison of computed and observed Schlumberger vertical electrical soundings

Due to the small area of investigation accurate regional gradient determination is impossible. Several lines (Figure 6) were extended so that the regional gradient could be determined.

The Elura prospect is in a regionally (gravity) flat area (Bureau of Mineral Resources Isogal Map, Cobar, 1:250,000, October 1970); the regional gradient could be approximated by a north-easterly dipping plane. Figure 7 illustrates the residual Bouguer anomaly. The residual anomaly is dominated by a large, almost circular, 13 μG positive anomaly centred to the north of the area. This anomaly widens into a significant low to the south.

Magnetic Curve Techniques and Constraints

A magnetic field anomaly may be defined as the superposition of a secondary magnetic field, caused by a variation in the total magnetic properties of the underlying rock, upon the main geomagnetic field. The magnetisation of rocks is due partly to induction in the earth's field and partly to their permanent (remanent) magnetisation. The induced intensity depends upon the magnetic susceptibility and the magnetising field while the remanent component has a complex dependence upon the type and amount of the magnetic minerals constituting the rock and also the events throughout the rock's history. Hence for a complete magnetic study, both must be studied.

The total intensity of the magnetic field was determined at 25 m intervals on the gravity grid using a Geometrics G816 proton precession magnetometer in which the detector head was 2 m above the ground surface. The accuracy of the field measurements is 2 nT. Readings at 5 m intervals were later recorded over the areas of interest.

The regional geomagnetic field for the Cobar area has an intensity of 57100 nT. Examination of the magnetic profiles suggests that a regional field of 57105 nT would be appropriate and that this level can be assumed to be constant over the surveyed area. This zero level has been re-

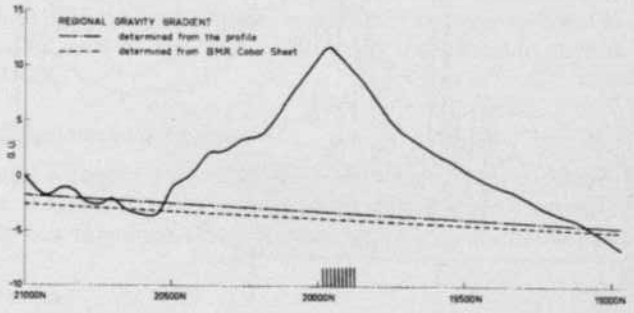

FIGURE 6

Extended gravity profile illustrating regional gradient. Line 20100E

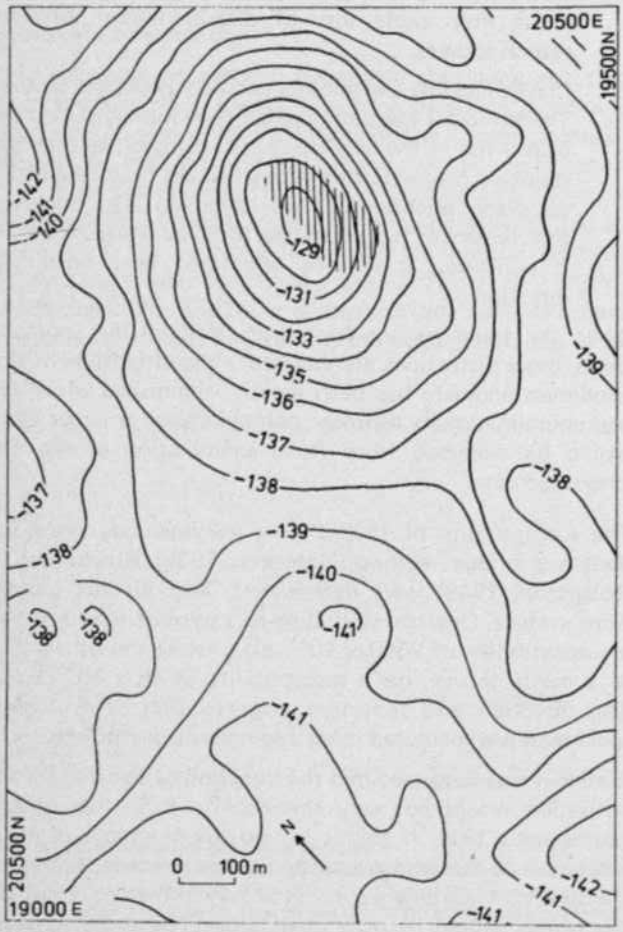

FIGURE 5

Bouguer anomaly. Contour interval 1 μG. Ore body indicated by hatching

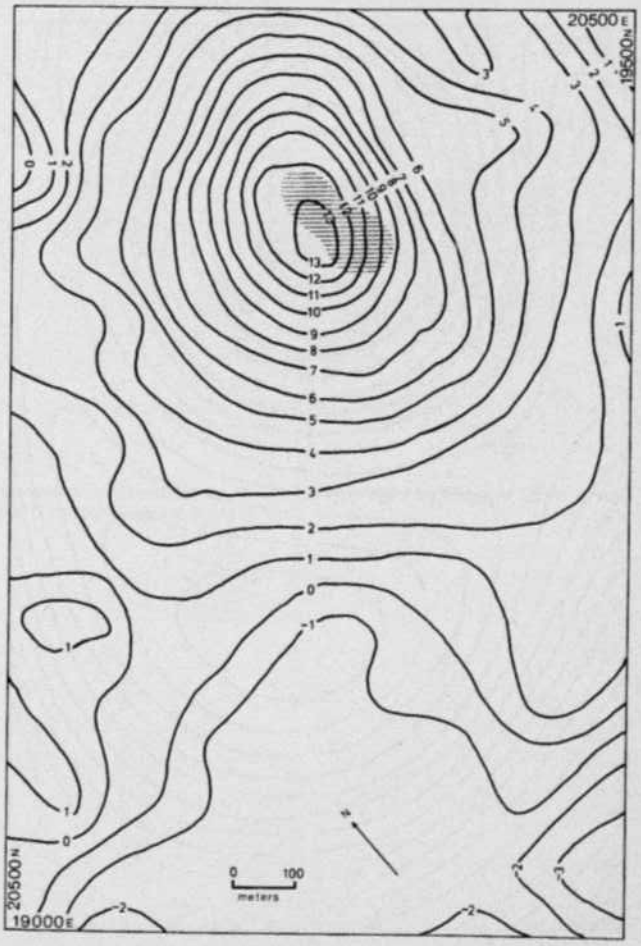

FIGURE 7

Residual Bouguer anomaly. Contour interval 1 μG

The directions of magnetisation of the core relative to the vertical axis of the core are illustrated in Figure 10. With the exception of one sample all points lie on the lower hemisphere. The upper hemisphere sample is thought to be due to the misorientation of the upward core axis direction. The points lie on a small circle of 10° and make an angle of 170 ° with the D.D.H. axis. The locus of points having an angle of 170° from the D.D.H. when plotted in its correct direction and dip attitude is illustrated by the solid line in Figure 10b. The position of the geomagnetic field is plotted and lies almost on this locus, so that the initial inference that the angle between the direction of magnetisation and the borehole axis should be the same as that between the D.D.H. and the geomagnetic field is justified.

The directions and intensities of magnetisation for various alternating demagnetising fields were determined. Alternating field demagnetisation greatly decreased the intensity of magnetisation while the direction was never far removed from that of the geomagnetic field. The effect of N.R.M. will therefore be minimal but nevertheless apparent.

Gravity and Magnetic Interpretation

The purpose of any interpretational method is to determine the most likely distribution of the anomalous mass causing the anomaly, which cannot be solved uniquely. However, the problem of calculating the potential field due to a known distribution of physical properties possesses a unique solution.

Downward continuation

A fundamental property of downward continuation is that when the disturbing masses have been passed by, continuation is no longer a valid solution of the inverse potential problem so that the solution becomes unstable and begins to oscillate and diverge. The onset of an instability indicates that a solution is being sought at too great a depth and so this method can be useful in gauging the limiting depth of the possible masses producing a given anomaly. Roy (1966) shows that there is another property of the continued field that may be utilised for inferring the depth to the top of an orebody. This is related to the rate at which the magnitudes of the maximum anomaly increase with the depth of continuation. He indicates that the depth of continuation corresponding to the point of maximum curvature of the maximum anomaly peak magnitude gives a very close indication to the limiting depth.

The continuation method at 25 m intervals has been applied to the field data and contoured (Figure 11). Semilog plots (Figure 12) of the maximum anomaly value against depth of continuation yields a depth to the top of the body of 77 m.

Downward continuation to a depth of 100 m elucidates possible body outlines. Indications are that to the grid east of 20100E on lines 20150E to 20250E two separate parallel bodies exist — the grid north body petering out before 20100E.

Total mass determination

Gauss's Theorem provides an elegant method for determining the magnitude of a mass producing a gravity anomaly without reference either to the shape or to the density of

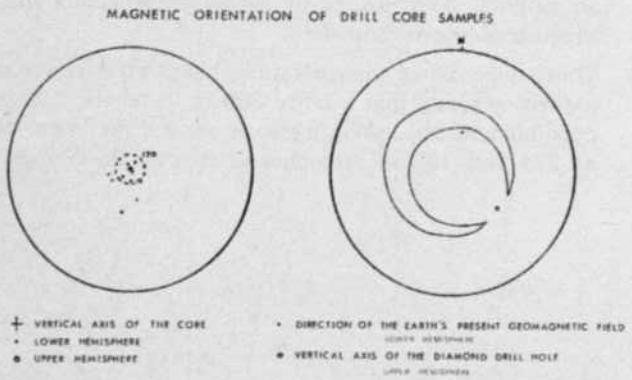

FIGURE 10

Magnetic orientation of drill core samples.
(a) Sterogram plot of the angle between the vertical axis of the drill core and the direction of magnetisation of the core sample. The dashed line shows the best fitting value for these angles.
(b) Sterogram plot of the D.D.H. axis. The crescentic line shows the locus of points making an angle of 170° to the D.D.H. axis. The direction of the earth's present geomagnetic field plots on this locus.

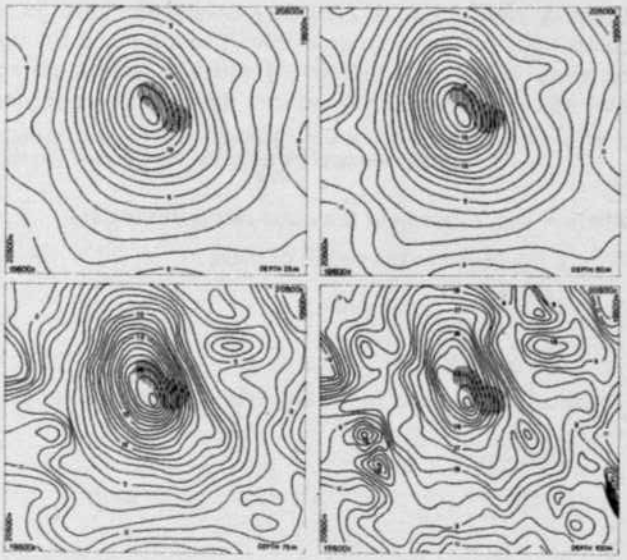

FIGURE 11

Downward continuations of the gravity field at Elura at 25 m intervals. Contour interval 1 μG

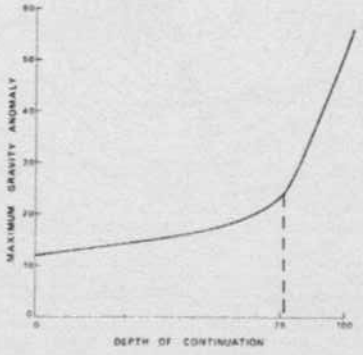

FIGURE 12

Magnitude of the maximum gravity anomaly (μG) versus depth of continuation (metres)

The directions of magnetisation of the core relative to the vertical axis of the core are illustrated in Figure 10. With the exception of one sample all points lie on the lower hemisphere. The upper hemisphere sample is thought to be due to the misorientation of the upward core axis direction. The points lie on a small circle of 10° and make an angle of 170 ° with the D.D.H. axis. The locus of points having an angle of 170° from the D.D.H. when plotted in its correct direction and dip attitude is illustrated by the solid line in Figure 10b. The position of the geomagnetic field is plotted and lies almost on this locus, so that the initial inference that the angle between the direction of magnetisation and the borehole axis should be the same as that between the D.D.H. and the geomagnetic field is justified.

The directions and intensities of magnetisation for various alternating demagnetising fields were determined. Alternating field demagnetisation greatly decreased the intensity of magnetisation while the direction was never far removed from that of the geomagnetic field. The effect of N.R.M. will therefore be minimal but nevertheless apparent.

Gravity and Magnetic Interpretation

The purpose of any interpretational method is to determine the most likely distribution of the anomalous mass causing the anomaly, which cannot be solved uniquely. However, the problem of calculating the potential field due to a known distribution of physical properties possesses a unique solution.

Downward continuation

A fundamental property of downward continuation is that when the disturbing masses have been passed by, continuation is no longer a valid solution of the inverse potential problem so that the solution becomes unstable and begins to oscillate and diverge. The onset of an instability indicates that a solution is being sought at too great a depth and so this method can be useful in gauging the limiting depth of the possible masses producing a given anomaly. Roy (1966) shows that there is another property of the continued field that may be utilised for inferring the depth to the top of an orebody. This is related to the rate at which the magnitudes of the maximum anomaly increase with the depth of continuation. He indicates that the depth of continuation corresponding to the point of maximum curvature of the maximum anomaly peak magnitude gives a very close indication to the limiting depth.

The continuation method at 25 m intervals has been applied to the field data and contoured (Figure 11). Semilog plots (Figure 12) of the maximum anomaly value against depth of continuation yields a depth to the top of the body of 77 m.

Downward continuation to a depth of 100 m elucidates possible body outlines. Indications are that to the grid east of 20100E on lines 20150E to 20250E two separate parallel bodies exist — the grid north body petering out before 20100E.

Total mass determination

Gauss's Theorem provides an elegant method for determining the magnitude of a mass producing a gravity anomaly without reference either to the shape or to the density of

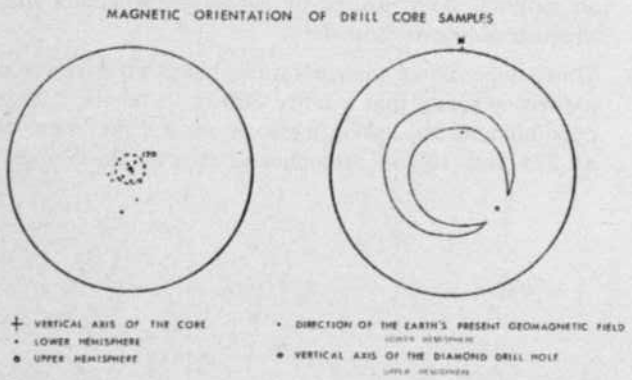

FIGURE 10

Magnetic orientation of drill core samples.
(a) Sterogram plot of the angle between the vertical axis of the drill core and the direction of magnetisation of the core sample. The dashed line shows the best fitting value for these angles.
(b) Sterogram plot of the D.D.H. axis. The crescentic line shows the locus of points making an angle of 170° to the D.D.H. axis. The direction of the earth's present geomagnetic field plots on this locus.

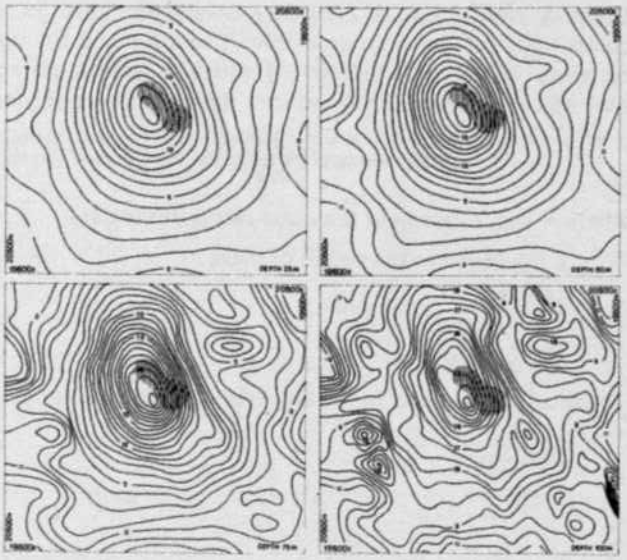

FIGURE 11

Downward continuations of the gravity field at Elura at 25 m intervals. Contour interval 1 μG

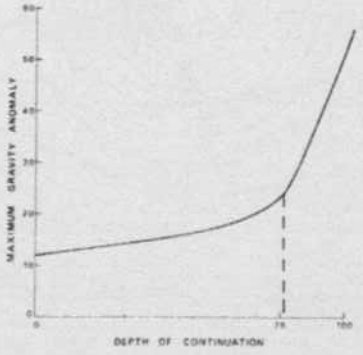

FIGURE 12

Magnitude of the maximum gravity anomaly (μG) versus depth of continuation (metres)

the anomalous body. It can be readily shown (Hammer, 1945; Goetz, 1958) that

$$\int_{-\infty}^{\infty} \int_{-\infty}^{\infty} \Delta g(x,y)dxdy = 2\pi\ GM \qquad (1)$$

where M is the excess mass and G is the gravitational constant.

Integrating under the gravity anomaly yields a value of $3.284 \times 10^6\ \mu G - m^2$ corresponding to an excess mass of 7.85×10^6 tonnes. In order to calculate the total "tonnage" we must multiply the excess mass by the ratio of the mineral density to the density contrast between the mineral and host rocks. Table 1 indicates the average mineral density to be 4200 kg/m^3 and that for the host rock is 2600 kg/m^3, so that the total mass of the disturbing body would be *20.6 x 10^6 tonnes.*

As this figure is critical in an economic assessment it is necessary to outline some possible pitfalls in its determination. Firstly, uncertainties in the amplitude of Δg occur in cases where a regional correction has been made. Secondly, the data exists only over a limited area, whereas in theory, the integrations are to be carried out over the entire horizontal plane.

Grant & West (1965, p. 270) have developed a method to compensate for the finitude of the integration and the uncertainty in the amplitude of Δg where a regional correction has been made. They reduced the problem to solving

$$4GM = \left(\tan^{-1} \frac{XY}{\bar{z}R}\right)^{-1} I \qquad (2)$$

where X and Y represent the outer limits of the data

$\bar{z}$ the depth to the centre of mass

$$I = \int_{-X}^{X} \int_{-Y}^{Y} \Delta g(x,y)dxdy$$

$$R = X^2 + Y^2$$

To calculate the term in the brackets we need to determine $\bar{z}$.

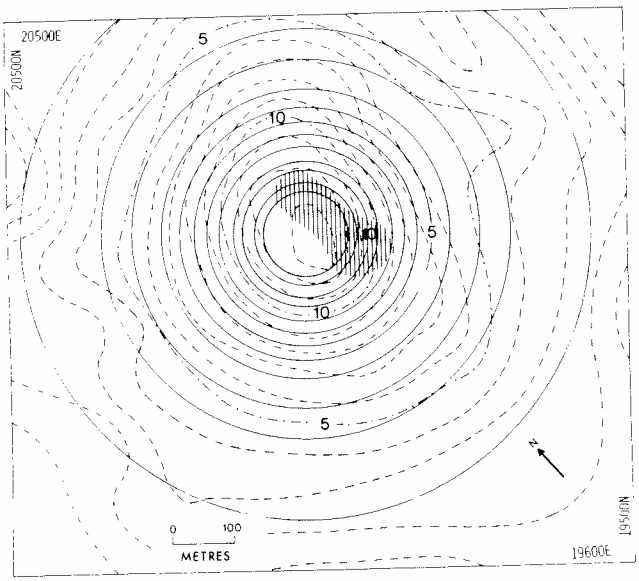

FIGURE 13

Comparison of the observed (dashed lines) and calculated (solid lines) gravity anomalies for a least squares best fitting spherical source. Contour interval 1 μG

The shape of the Bouguer anomaly contours suggests that the body may well be represented by a sphere. An iterative procedure which makes use of an algorithm proposed by Marquardt (1963) has been developed. This program computes the least squares estimate for the co-ordinates of the centre of the sphere which were 19970N, 20146E, and 209 m below the ground surface. A comparison between the observed and calculated anomalies (Figure 13) shows reasonable correlation, especially along the profiles near the co-ordinates of the centre of the mass. By a similar procedure one can determine the least squares fit for a magnetised spherical body in which all the magnetisation is induced and oriented in the direction of the undisturbed field. Least square fitting of 295 sample points (Figure 14) has determined the co-ordinates for the centre of mass as 20165E, 19978N and a depth to the centre of the body of 194 m. The close correlation between the predicted co-ordinates for the centre of mass for both the magnetic and gravity procedures implies a similar causative source.

Assuming $\bar{z}$ = 210 m yields an excess mass of 12.7×10^6 tonnes which corresponds to a total mass of 33.4×10^6 tonnes for the disturbing body if a mineral density of 4200 kg/m^3 is assumed. This figure is similar to that determined by Hammer's method.

Locating the Centre of Mass

Grant & West (1965, p. 228) show that the centre of mass of a disturbing body of mass M, on the plane z = 0, may be found by solving the following expressions

$$\int_{-\infty}^{\infty} \int_{-\infty}^{\infty} x\ \Delta g(x,y)dxdy = 2\pi\ GM\bar{x} \qquad (3)$$

$$\int_{-\infty}^{\infty} \int_{-\infty}^{\infty} y\ \Delta g(x,y)dxdy = 2\pi\ GM\bar{y} \qquad (4)$$

where x and y are the x and y co-ordinates of the centre of mass. Having calculated M in the previous section, $\bar{x}$ and $\bar{y}$ can now be determined. For this anomaly the centre of mass is at 19993N, 20136E.

Three Dimensional Model

Talwani & Ewing (1960) and Talwani (1965) have derived expressions for the gravitational and magnetic attraction at an external point caused by a horizontal lamina with an irregular polygonal boundary.

Three dimensional interpretation, based on trial and error models, suggests that a body 300 m in length, 120 m in maximum width, having a maximum and minimum depth of 374 and 108 m respectively, striking 25°W from the

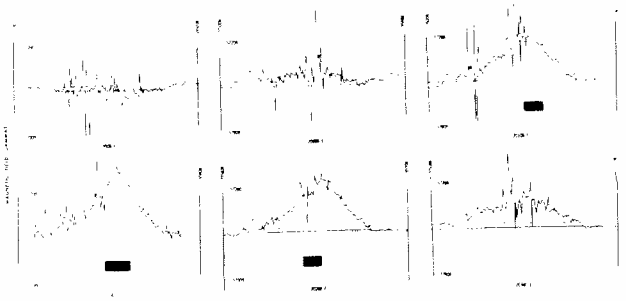

FIGURE 14

Comparison of the observed (continuous line) and calculated (points) total magnetic anomalies for a least squares best fitting spherical source. Units nT. Orebody position indicated by bars

survey baseline (20000N) and dipping at 78° grid north west best satisfies the gravity and magnetic anomalies. Due to the poor resolution of the bottom of the body the maximum depth is subject to large error. A block diagram of the anomalous mass is illustrated in Figure 15 while the observed and computed gravity profiles (Figure 16) and magnetic profiles (Figure 17) are shown. This three dimensional body has a volume of 8.20 x 10^6 m^3 corresponding to a mass of 34.4 x 10^6 tonnes assuming a density of 4200 kg/m^3.

Summary and plausibility of the model

Direct and indirect gravity and magnetic interpretation for the Elura anomaly suggests a body 300 m in length, 120 m in maximum width and 266 m thick, centred at 19993N, 20136E, striking at 25° to the survey baseline and dipping at 80° grid north west with a total volume of 8.20 x 10^6 m^3 and mass of 34.4 x 10^6 tonnes. It is necessary to ask if such a body is geologically plausible. The characteristics of the Elura massive sulphides suggest a Cobar-type ore. As mentioned earlier the Cobar orebodies have steeply pitching pipe-like forms with great vertical persistence. Kappelle (1970) illustrates cross-sections of the C.S.A. mine which also shows much similarity to the three dimensional model.

Electromagnetic Survey

Electromagnetic dip angle measurements were made using a dual frequency (1000 Hz and 5000 Hz) McPhar vertical loop E.M. System powered by a portable engine-driven a.c. generator. With this system the transmitting coil is mounted, with its plane vertical, as close to the conductor axis as possible and oriented towards the receiving coil which occupies successive stations on traverse lines across the strike of the conductor. The transmitting coil was located at 20000N, 20100E and the receiving coil was moved along lines 20000E, 20050E, 20100E, 20200E. The tilt angle anomalies are illustrated in Figure 18.

Conclusions

The Elura deposit was discovered by application of routine geophysical methods. Preliminary interpretation of a reconnaissance aeromagnetic survey revealed an anomalous spherical body centred 250 m below the surface and having

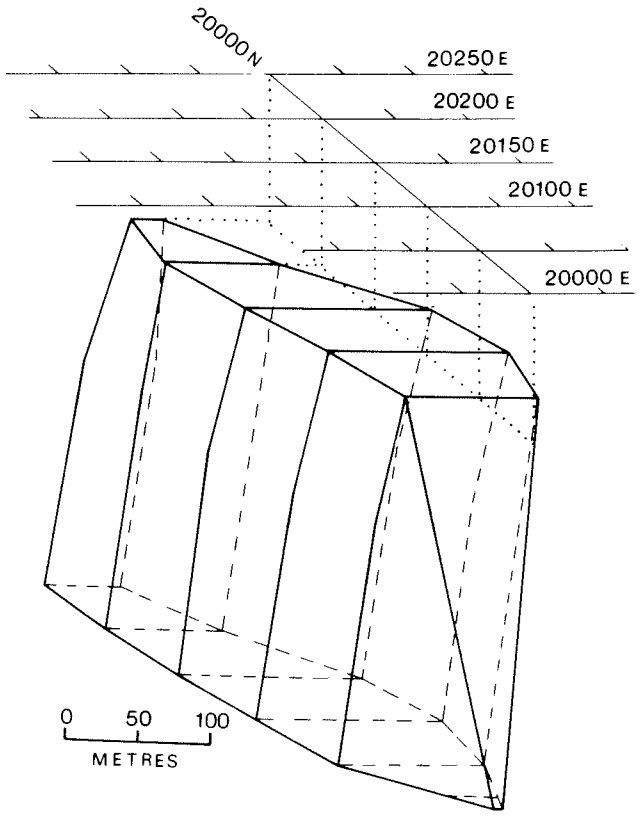

FIGURE 15

Three dimensional interpretive model for the Elura model

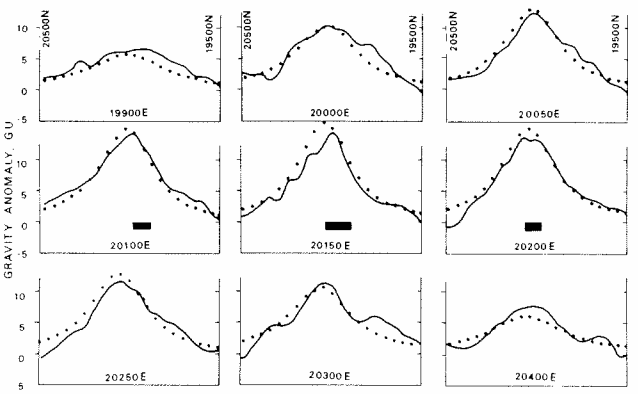

FIGURE 16

Comparison of the observed (solid lines) and computed (dots) gravity anomaly for the three dimensional model

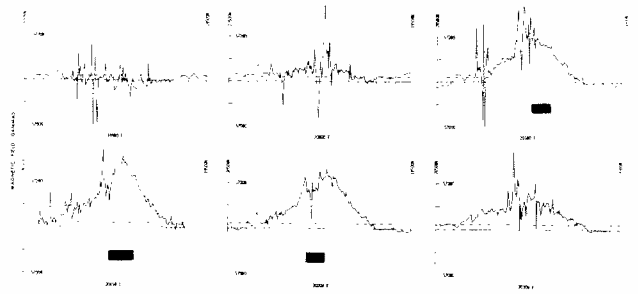

FIGURE 17

Comparison of the observed (solid lines) and computed (dots) total magnetic anomaly for the three dimensional model

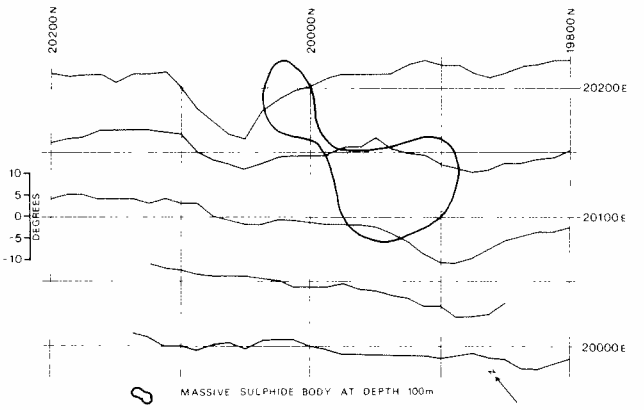

FIGURE 18

Tilt angle vertical loop E/M anomaly at Elura – loop centred at 20100E, 20000N, frequency 1000 Hz

a radius of 71 m. Ground magnetic, gravity, E.M., I.P. and resistivity surveys have confirmed this source.

Three dimensional magnetic and gravity interpretation suggests a source 300 m in length, 120 m in maximum width, having a maximum and minimum depth of 374 and 108 m respectively, and a volume of 8.20×10^6 m^3 corresponding to a mass of 34.4×10^6 tonnes. Visual inspection of the Bouguer anomaly contour plot indicates the body strikes 25° grid north of the survey base line (20000N). Data from gravity and magnetic surveys suggests that this body is centred at 20140E, 19980N. Magnetic orientation of three banded massive sulphide drill core specimens shows that the banding strikes at about this angle and dips at approximately 80° grid north west — as predicted by the gravity interpretation.

References

BLACKBURN, G. J., 1974. Geophysical studies at Elura, Cobar: unpub. B.Sc. Honours thesis, University of Tasmania.

BLACKBURN, G. J., 1980. Elura orebody, Australia — a case history: unpub.

BRUCKSHAW, J., and ROBERTSON, E. I., 1948. The measurement of magnetic properties of rocks. *J. Sci. Instr.*, v. 25, p. 444.

GOETZ, J. F., 1958. A gravity investigation of a sulphide deposit. *Geophysics*, V. 23 (3), 606-623.

GRANT, F. S., and WEST, G. F., 1965. *Interpretation Theory in Applied Geophysics.* New York, McGraw-Hill.

GREEN, R., 1961. The adjustment of misclosures in networks with special reference to microbarograph surveys. *Cartography*, v. 4, 36-40.

GUSTARD, B., and SCHUELE, W. J., 1966. Anomalously high remanence in $(\gamma\text{-}Fe_2O_3)_{1-x}$ and $(\alpha\text{-}Fe_2O_3)_x$ particles. *J. Appl. Phys.*, v. 37, 1168-1170.

HAMMER, S., 1945. Estimating ore masses in gravity prospecting. *Geophysics*, V. 10 (1), 50-62.

JOHNSON, E. A., 1935. The limiting sensitivity of an alternating current method of measuring small magnetic moments. *Rev. Sci. Instr.*, v. 9, p. 263.

KAPPELLE, K., 1970. Geology of C.S.A. mine, Cobar, N.S.W. *Proc. Aust. Inst. Min. Metall.*, v. 233, 79-94.

MARQUARDT, D. W., 1963. An algorithm for least squares estimation of non-linear parameters. *J. Soc. Indust. Appl. Math.*, v. 11 (2), 431-442.

MOONEY, H. M., ORELLANA, E., PICKETT, H., and TORNHEIM, L., 1966. A resistivity computation method for layered earth models. *Geophysics*, v. 31 (1), 192-302.

RICHARDSON, L. A., and KEATING, W. D., 1947. Preliminary report on a geophysical survey at Cobar, N.S.W.: unpub. report, Geological Survey of N.S.W., G.S. 1947/038.

ROY, A., 1966. The method of continuation in mining geophysical interpretation. *Geoexploration*, v. 4, 65-83.

TALWANI, M., 1965. Computation with the help of a digital computer of magnetic anomalies caused by bodies of arbitrary shape. *Geophysics*, v. 30 (5), 797-817.

TALWANI, M., and EWING, M., 1960. Rapid computation of the gravitational attraction of three dimensional bodies of arbitrary shape. *Geophysics*, v. 25 (1), 203-225.

THOMSON, B. P., 1953. Geology and ore occurrence in the Cobar district. Geology of Australian Ore Deposits, Publs. 5th Emp. Min. Metall. Congr. Aust. N.Z., v. 1, 863-896.

YUNGUL, S., 1956. Prospecting for chromite with gravimeter and magnetometer over rugged topography in eastern Turkey. *Geophysics*, v. 21 (2), 433-454.